Evaluation of ground vibrations induced by blasting in a limestone quarry

Punit Paurush and Piyush Rai*

Department of Mining Engineering, Indian Institute of Technology, Banaras Hindu University, Varanasi 221 005, India

Despite being a versatile and low-cost method, rock blasting produces undesirable severe effects. The present study aims to examine the ground vibrations produced by blasting, which are of serious concern to mine operators as well as the nearby inhabitants. Forty-nine field-scale trial blasts were conducted and recorded to measure ground vibrations produced by blasting in a limestone quarry in Rajasthan, India. The multivariate linear regression (MLR) and artificial neural network (ANN) techniques were used to predict the peak particle velocity (PPV) with distance between the blasting site and measuring station, charge per delay and scaled distance as the input parameters. Subsequently, a coefficient of determination (R^2) was calculated using MLR and ANN approaches. Additionally, to verify whether the recorded events exceeded the threshold levels, the values of PPV and dominant frequency propounded by the United States Bureau of Mines (USBM), German standard (DIN), and Director General of Mines Safety, India were carefully scrutinized. Results were compared based on R^2 values obtained by the USBM predictor equation, MLR and ANN techniques. It was found that ANN provided a good prediction with a high degree of correlation (0.901) in comparison to MLR (0.754). Also, frequency analysis for the study field showed that the dominance of frequencies was in the range 10–40 Hz. Although the values were within safe limits, disturbances may be witnessed in nearby structures if PPV values are high at lower frequency range.

Keywords: Blasting, ground vibration, limestone quarry, peak particle velocity, threshold levels.

BLASTING is one of the most economical methods used for fragmenting rock mass. However, rock blasting causes several undesirable effects, such as ground vibrations, air overpressure, flyrocks, dust hazards, etc. It is consequential to mention that merely 20%–30% of the explosive energy is used to fragment and displace the rock mass, while the rest is dissipated in the form of ground vibrations, air blasts, noise and flyrocks, etc.[1].

Ground vibrations due to blasting in surface mines are one of the basic concerns in the mining industry, and predicting it can be helpful in the minimization of environmental problems. Generally, blasting-induced ground vibrations damage the free faces and cause backbreaks. These backbreaks hinder the drilling operations for subsequent blast bounds and lead to improper blasting with excessive fines or generate over-sized boulders. This negatively impacts the economics of the mines, delays the production and weakens the socio-economic development of the surrounding areas. Therefore, it is important to control and predict the ground vibrations with precision. Further, uncontrolled ground vibration and frequencies are of significant concern as they may damage the existing surface structures and cause nuisance to residents in the vicinity of the mines. In recent years, environmental issues induced by blasting activities have become one of the most important concerns[2–7].

Regulations on ground vibrations focus primarily on peak particle velocity (PPV), which has been studied by various researchers[8–12]. The United States Bureau of Mines (USBM) established the first PPV predictor equation. Modified predictors from other researchers and institutions[13–16]. However, the PPV predictor equation of USBM is still the most popular one.

Some predictive state-of-the-art techniques like artificial natural network (ANN) and multivariate linear regression (MLR) have been used to assess blast effectiveness[17–21]. If there are concerns about damage due to blasting vibrations, several defined damage criteria (USBM, DIN 4150 and Directorate General of Mines Safety (DGMS)) can be used for analysis[22–24].

The present study aims to predict ground vibrations by developing the predictor equations using ANN and MLR-based statistical techniques for a limestone quarry in Rajasthan, India. The key objectives of this study are as follows:

(1) To determine the site-specific constants (K and β) for the quarry using statistical analysis and to develop the predictor equations for PPV.

(2) To predict PPV using the MLR and ANN techniques and compare the value of coefficient of determination (R^2) obtained by each method.

(3) To compare the recorded PPV and frequency values with the established damage criteria of USBM, DIN 4150 and DGMS.

Site description

The trial blasts were carried out in an open-cast limestone quarry in Rajasthan. The limestone formation in the quarry

*For correspondence. (e-mail: prai.min@itbhu.ac.in)

Table 1. Salient properties of limestone formation

Age, group and period	Dip direction of the formation	Chemical composition (%)	Texture and colour	Hardness
Lower Vindhyan age, Khori group and Tertiary period	0° to 20° towards east–west	CaO: 42–44 MgO: 1–2 SiO_2: 14–18 Al_2O_3: 0.2–0.6 Fe_2O_3: 0.1–0.5	Light to dark grey. Granular texture	Soft to moderately hard (2.5–4 on Mho scale of hardness)

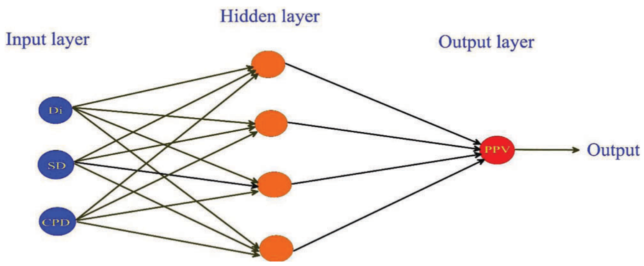

Figure 1. Structure of a three-layer, feed-forward multilayer perceptron (MLP) model.

is mainly constituted of sedimentary carbonate rocks, which are usually skeletal fragments of marine organisms. The formation was of Eocene age in the tertiary period. The limestone was hard and compact with low silica content. The deposit belongs to the Nimbahera limestone formation. Table 1 shows the salient properties of this formation. Limestone, shale and clay were the major rock types of this formation. The deposit was fine-grained and massive in structure. It was exposed to structural disturbances of very subdued magnitude, as evidenced by minor folds and joints.

Background

Approaches used for PPV prediction

USBM predictor equation-based approach: Ground vibrations are characterized by the measurement of PPV to estimate the potential damage. PPV depends mainly on the maximum charge, distance between the blast and the measuring point, and is highly dependent on the ground characteristics[25]. PPV is related to the maximum charge per delay (CPD) and distance by the predictor equation established by USBM (eq. (1)), which is the most commonly used relationship for its estimation.

$$\text{PPV (mm/s)} = K \times \left(\frac{D}{\sqrt{W}}\right)^{-\beta}, \tag{1}$$

where D is the distance between the blasting and measuring points (m), W the maximum CPD (kg) and $(D/\sqrt{W})$ is the scaled distance (SD; m/kg$^{1/2}$).

K and β are the site constants to be determined by regression analysis, and are dependent on ground characteristics.

MLR analysis: This method is used to model the linear relationship between a dependent variable and one or more independent variables[26]. It is based on the least-squares method and aims to minimize the sum of squares of the predicted and measured values. The MLR technique-based PPV prediction has been made in this study.

ANN using multi-layer perceptron: ANN is a type of artificial intelligence based on the neuronal system of humans. There is a wide range of possibilities for solving ANN problems, particularly for the approximation of nonlinear behaviour without prior knowledge of inter-relationships between elements within a system[27]. An ANN is a highly integrated computational network of basic information processing components known as neurons or perceptrons. One of the most commonly applied ANNs is the multilayer perceptron (MLP) technique, which has been widely used by numerous researchers to predict ground vibrations[28–30].

Figure 1 shows the structure of the MLP model to meet the research objectives. It is a supervised model using feed-forward architecture and can have multiple hidden layers. The MLP layers have different functions. The interface layer on input side of the network is known as the sensory layer (or the common input layer); the one on the display side is called the output layer. All intermediate layers are referred to as hidden layers.

MLP uses an iterative routine for gradient-based optimization called back-propagation (BP) learning technique[31]. The back-propagation algorithm performs learning on a multi-layer feed-forward neural network. Each layer is made up of units called perceptrons. The inputs to the network correspond to the attributes measured for each training step. The inputs are fed simultaneously into the units making up the input layer. These inputs pass through the input layer and are then weighted and fed simultaneously to the second layer of perceptrons, known as a hidden layer. The outputs of the hidden layer units can be input to another hidden layer and so on. The number of hidden layers is arbitrary, although only one is used in practice. The weighted outputs of the last hidden layer are input to units making up the output layer, which provide the network's prediction for a given training. It is a feed-forward network since none of the weights cycles back to an input unit or to a previous layer's output unit. It is fully connected in that each unit provides the input in the next forward layer.

Table 2. Regulatory limits of ground vibration according to United States Bureau of Mines (USBM) and DIN criteria

USBM-RI8507			DIN-4150			
	PPV (mm/s)			PPV (mm/s)		
Structure	<40 Hz	≥40 Hz	Structure	10 Hz	10–50 Hz	50–100 Hz
Modern homes – dry	18.75	50	Industrial buildings	20	20–40	40–50
Wall interiors			Residential buildings	5	5–15	15–20
Older homes	12.75	50	More sensitive buildings	3	3–8	8–10

PPV, Peak particle velocity.

Table 3. Safe blasting limits according to Directorate General of Mines Safety (DGMS)

	Dominant excitation frequency (Hz)		
Type of structure	<8	8–25	>25
Building/structures not belonging to the owner			
Domestic houses/structures	5	10	15
Industrial buildings	10	20	25
Sensitive structures/buildings	2	5	10
Buildings belonging to the owner during a limited span of time			
Domestic houses/structures	10	15	25
Industrial buildings	15	25	50

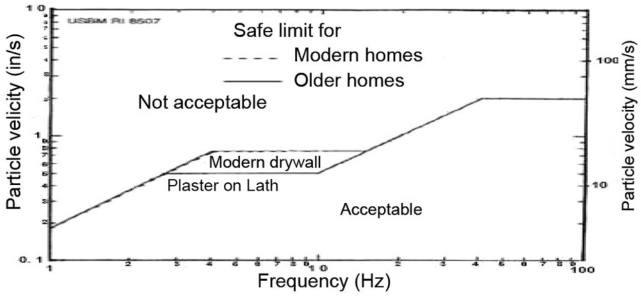

Figure 2. Safe blasting limits (United States Bureau of Mines (USBM) approach).

The perceptron inputs are weighted by a corresponding weight (w). The weight of the inputs and the bias (b) constitute the input for the activation function f (ref. 32). The output (y) can be expressed in terms of activation function as given in eq. (2).

$$y = f\left(\sum_{i=1}^{N} w_i x_i + b\right), \tag{2}$$

where x_i is the ith input, w_i the weight associated with the ith input, b the bias and f is the activation function of the perceptron.

Regulatory limits on blast-induced ground vibrations and frequencies

It has been established that the particle velocity of ground motion near structures is an effective criterion for the assessment of damage. According to USBM RI 8507, PPV provides the best description for ground vibrations[33].

Over the last more than two decades, PPV and frequency have been together used for assessment of damage due to blasting. Accordingly, the USBM and DIN regulatory standards were developed (Table 2). Thus, if the recorded PPV values at a specific predominant frequency lay below the solid line (Figure 2), then PPV may be considered safe (USBM approach). DIN 4150 provides three lines for time-dependent vibration limits for different structures (Figure 3)[25,33–35]. The first line (line 1) is used for buildings, mostly for commercial and industrial purposes. The second line (line 2) is associated with a similar design for dwellings and buildings. The third line (line 3) is often used for structures not included under lines 1 and 2, due to their intrinsic sensitivity to vibration. The potential damage at a low-frequency range (<40 Hz) is significantly higher than that at a high-frequency range (>40 Hz). This is due to the effects of resonance at the natural frequency of the structures and buildings that fall in between 5 and 16 Hz (ref. 36). Hence, if the values of PPV are plotted in conjunction with frequency and they fall within the inner region, where the frequency is always greater than 40 Hz, it is considered safe.

According to the Indian standard as specified by the DBMS, Table 3 shows the regulatory limits in terms of PPV and frequency of ground vibrations[37]. Therefore, it is implicit that for a thorough study of blasting vibrations, measurement of frequency as well as PPV is essential.

Research methodology

The research methodology adopted here includes the conduct of real-time trial blasting and measurement of PPV and frequency. In the present study, a total of 49 trial-blasting

Table 4. Input and output parameters for analysis

Blast no.	Distance (m)	Charge per delay (CPD, kg)	Scaled distance (SD, m/kg$^{1/2}$)	PPV (mm/s)	Frequency (Hz)
B1	140	50	19.80	5.2	30
B2	140	47.26	20.36	5.8	27
B3	150	50	21.21	5.3	24
B4	150	44.48	22.49	4.8	22
B5	150	47.26	21.82	5.1	21
B6	150	47.26	21.82	5.2	47
B7	160	41.7	24.78	4.8	27
B8	170	47.26	24.73	4.62	16
B9	170	44.48	25.49	3.6	47
B10	175	47.26	25.46	4.1	20
B11	190	47.26	27.64	3.6	32
B12	190	40.3	29.93	3.5	23
B13	200	44.48	29.99	1.9	12
B14	200	47.26	29.09	4.2	32
B15	210	80.2	23.45	3.2	64
B16	210	50.2	29.64	3.6	31
B17	210	40.3	33.08	3.2	15
B18	210	47.26	30.55	2.9	34
B19	240	51.63	33.40	2.1	32
B20	240	40.6	37.67	1.7	43
B21	240	59.57	31.10	4.1	34
B22	240	51.4	33.48	1.9	23
B23	250	40.6	39.24	1.9	26
B24	250	40.6	39.24	2.5	24
B25	260	50.2	36.70	2.1	64
B26	280	50.2	39.52	1.4	10
B27	280	50.2	39.52	1.6	32
B28	290	50.05	40.99	1.6	30
B29	290	51.63	40.36	2.1	20
B30	290	42.6	44.43	2.5	20
B31	293	40.3	46.15	1.5	20
B32	300	42.6	45.96	1.3	25
B33	300	43.2	45.64	1.3	57
B34	309	54.96	41.68	1.4	32
B35	310	48.03	44.73	1.3	21
B36	310	30.1	56.50	1.2	2
B37	310	50.2	43.75	1.6	32
B38	310	43.1	47.22	1.2	20
B39	310	42.3	47.66	1.3	40
B40	320	46.2	47.08	1.4	34
B41	340	50.4	47.89	1.7	12
B42	350	50	49.50	1.5	10
B43	350	44.29	52.59	1.3	17
B44	350	80.2	39.08	1.5	20
B45	350	40.5	55.00	1.1	43
B46	360	29.74	66.01	1.1	12
B47	360	43.94	54.31	1.1	24
B48	370	76.39	42.33	1.3	18
B49	400	82.21	44.12	1.4	33.33

CPD, Change per delay; SD, Scaled distance; PPV, Peak particle velocity.

rounds were implemented and recorded (Table 4). For this, the seismographs were placed at fixed distances from the blasting site.

In order to determine the site-specific parameters (K and β), regression analysis was used for the measured PPV and SD. Subsequently, the value of R^2 between PPV and SD was obtained using regression analysis and a graph was plotted between PPV and SD. The MLR technique was then used to establish the connection between the input and output parameters for developing the predictor equation as follows

$$\overline{Y} = a + b_1X_1 + b_2X_2 + \ldots + b_nX_n, \quad (3)$$

where $\overline{Y}$ is predicted value of Y, a the intercept and b is the partial regression coefficient.

For this prediction, three parameters, namely D_i, CPD and SD, were selected as input parameters and PPV as the output parameter.

To further substantiate the results, ANN (MLP) was used to predict PPV. The MLP module was used to build the neural network model. The MLP neural networks were trained using a back-propagation algorithm to update weights to reduce the error function. Out of 49 trial-blasting datasets, about 70% were used for training and 30% were assigned for testing. In the present ANN module, the training datasets provided the weights for building the model, while the testing datasets identified the errors and prevented overtraining.

To predict PPV (output), three input parameters were used, namely D_i, CPD and SD, both for MLR and ANN techniques. Subsequently, R^2 was determined. The values of R^2 obtained using the generalized predictor equation, MLR and ANN approaches were carefully scrutinized.

Further, the PPV and frequency values of all 49 trial blasts were evaluated in light of the USBM, DIN and DGMS criteria in order to properly ascertain the damage risk of the nearest buildings and structures.

Table 5. Descriptive statistics of the parameter

Parameter	No. of data	Minimum	Maximum	Mean
Distance	49	140	400	257.69
CPD	49	29.74	82.21	48.61
SD	49	19.79	66.01	37.43
PPV	49	1.10	5.80	2.56
Frequency	49	2.00	64.00	27.63

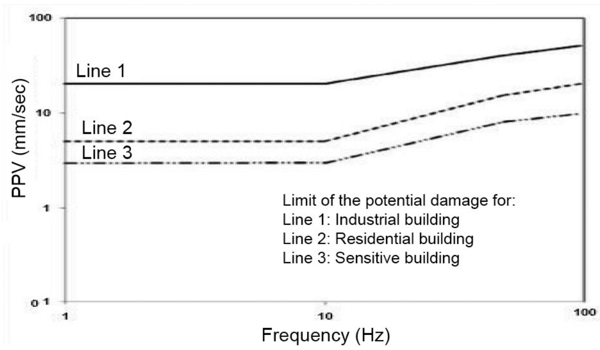

Figure 3. Safe blasting limits (DIN 4150 approach).

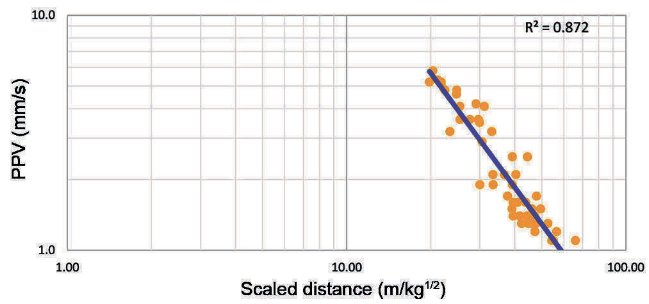

Figure 4. Relationship between peak particle velocity (PPV) and scaled distance (SD).

Results and discussion

Table 5 shows the primary descriptive statistics of all the input and output parameters of the study, together with their symbols. The salient results obtained from this study are discussed below.

Determination of predictor equation using the USBM method

The measured ground vibration datasets, including PPV and SD for the blasts were statistically analysed to determine the site constants (K and β) of the USBM predictor equation for the quarry. The predictor equation developed using the statistical analysis is given in eq. (4).

$$\mathrm{PPV} = 715.76 \times \mathrm{SD}^{-1.615}, \quad (R^2 = 0.8762). \tag{4}$$

The site constants K and β were determined by regression analysis and their values were 715.76 and –1.615 respectively.

The value of 0.872 (R^2) indicates that 87.2% of PPV variability is explained by regression analysis. Figure 4 shows the relationship between PPV and SD on a log–log diagram.

Prediction of PPV by the MLR technique

The predictor equation for PPV (output parameter) in terms of input parameters (D_i, CPD and SD) was obtained using the MLR technique. The MLR-based predictor equation is given as follows

$$\mathrm{PPV} = 6.018 - D_i \times 0.020 + \mathrm{CPD} \times 0.026 + \mathrm{SD} \times 0.012. \tag{5}$$

The value of R^2 was obtained and Table 6 provides the model summary. The predicted PPV value was plotted against its measured value (Figure 5). It is evident from Figure 6 that the predicted values of PPV using the MLR technique are almost similar to the observed values. The value of R^2 determined by the MLR technique was found to be 0.754, which shows 75.4% authenticity of PPV prediction.

Table 6. Model summary of multi-variate linear regression (MLR)

R	R-square	Adjusted R-square	Standard error of the estimate
0.868	0.754	0.726	0.6184450

Prediction of PPV by ANN technique

To perform the MLP neural network analysis, D_i, CPD and SD were selected as input parameters and PPV as the output parameter. Table 7 provides the ANN model processing summary. The ANN architecture has three nodes for the input layer, three nodes for the hidden layer and one node for the output layer. Activation function was the hyperbolic tangent and identity function for hidden and output layers respectively. Sum of errors was used as the error function in the said architecture. Figure 7 shows the network diagram to predict PPV.

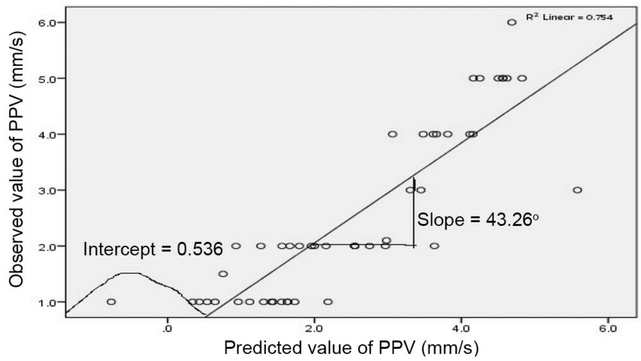

Figure 5. Plot between observed and predicted PPV values using multi-variate linear regression (MLR) technique.

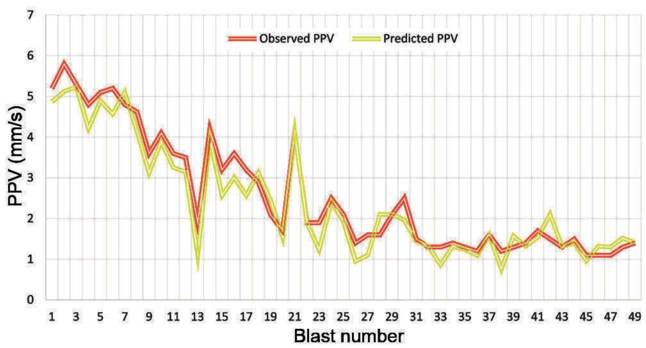

Figure 6. Comparison curve for observed and predicted PPV values using MLR technique.

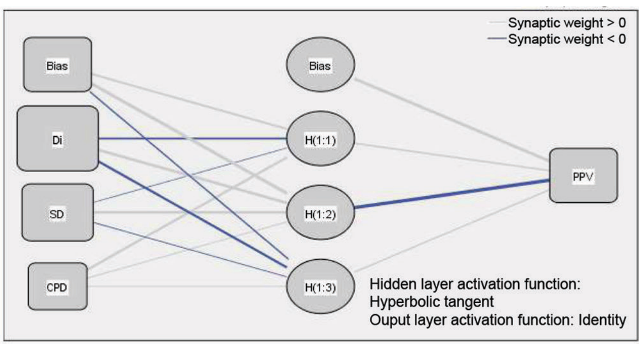

Figure 7. Network diagram to predict PPV.

The model summary presented in Table 8 provides information related to the results of training and testing samples. Sum of square errors is given for both training and testing samples. Very low magnitude of sum of square error in the training and testing datasets indicates the power of the model to predict the outcome. As revealed in Table 8, the sum of square error is 0.918% for the training dataset and 1.241% for testing dataset.

The predicted values of PPV were plotted against its measured values (Figure 8). It is evident from Figure 9 that the predicted and observed values of PPV by the ANN method are almost similar. This is indicative of a good prediction of PPV by the ANN method. The value of R^2 was found to be 0.901.

The MLP-based neural network model also provided information about the impact of each independent variable

Table 7. Model processing summary of artificial neural network (ANN)

	N	Percentage
Sample		
Training	33	67.3
Testing	16	32.7
Valid	49	100.0
Excluded	0	
Total	49	

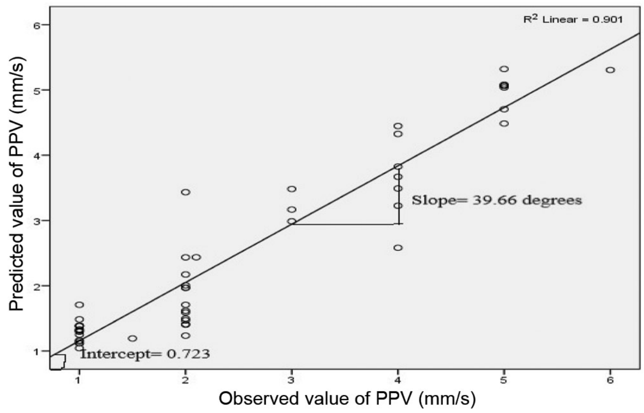

Figure 8. Plot between observed and predicted PPV values using artificial neural network (ANN) technique.

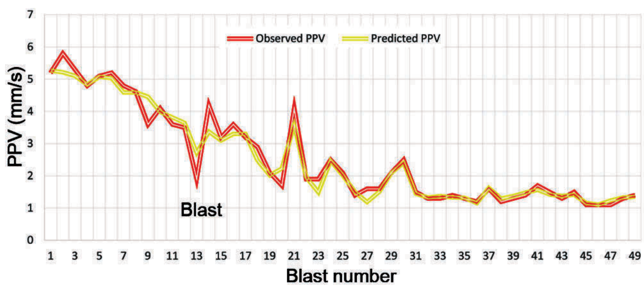

Figure 9. Comparison curve for observed and predicted PPV values using MLR technique.

Table 8. Model summary of the ANN

Training	Sum of square error	0.918
	Relative error	0.057
	Stopping rule used	One consecutive step(s) with no decrease in error
Testing	Sum of square error	1.241
	Relative error	0.188

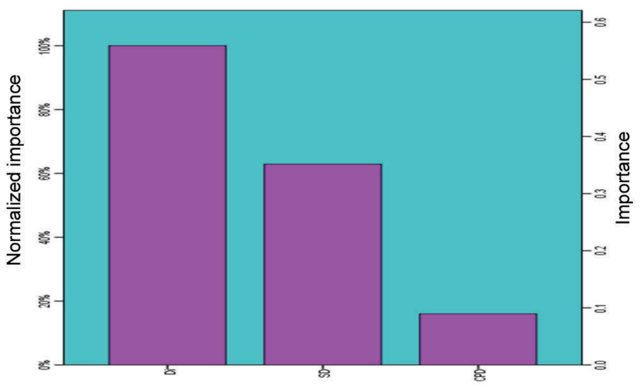

Figure 10. Relative importance of distance (D_i), SD and charge per delay (CPD).

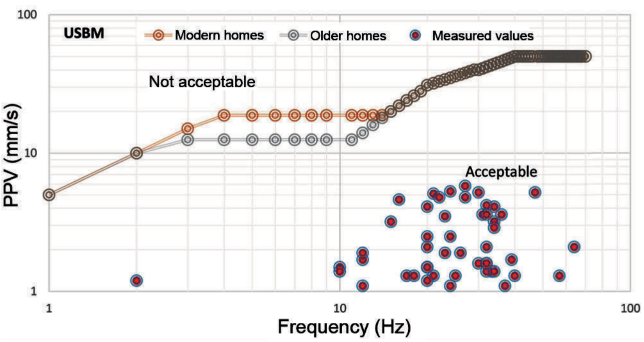

Figure 11. Damage risk assessment of the measured datasets according to USBM criterion.

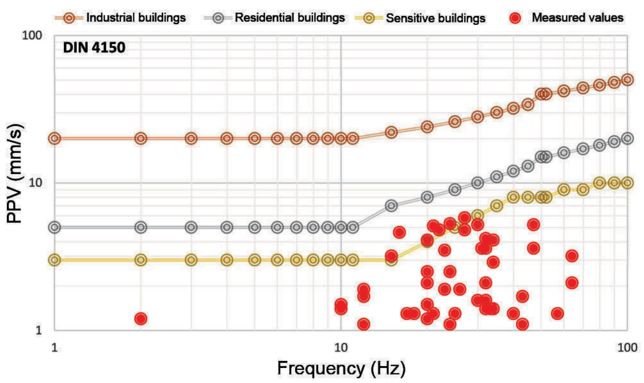

Figure 12. Damage risk assessment of the measured datasets according to DIN 4150 criterion.

in terms of their normalized importance. Figure 10 reveals the importance of the input (independent) variables. It can be inferred from Figure 10 that CPD has the lowest

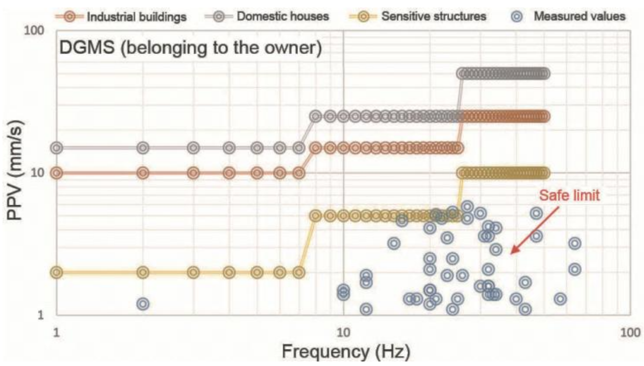

Figure 13. Damage risk assessment of the measured datasets according to DGMS (belonging to the owner) criterion.

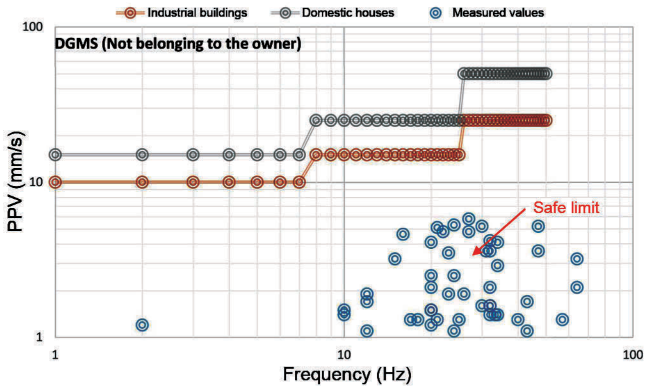

Figure 14. Damage risk assessment of the measured datasets according to Director General of Mines Safety (not belonging to owner) criterion.

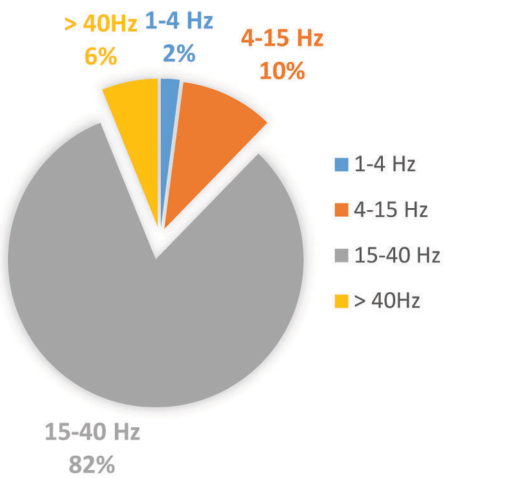

Figure 15. Pie chart for the frequency of the studied blasts.

impact on PPV. This implies that the explosive charge in various blast rounds has been well-designed. The greater impact of D_i and SD naturally implies the importance of ground conditions on PPV.

Results of damage risk assessment for the studied blasts

It is evident from Figures 11–14 that the PPV values for the trial blasts place almost all of them (excepting one with low frequency of 2 Hz) under the safe and acceptable category vis-à-vis various damage criteria assessment standards.

Results of frequency analysis

The classification of recorded frequency values from the study mine is shown in Figure 15 as a pie chart.

From Figure 15, it may be observed that only 2% of the measured frequencies lie in range 1–4 Hz, 10% in the range 4–15 Hz, 82% in the range 15–40 Hz and 10% in the range 4–15 Hz. Therefore, it may be interpreted from an Indian as well as global perspective that the PPV values vis-à-vis dominant frequencies in the study blast are safe.

The present methodology and the proposed equation can be used for other sites with similar ground characteristics.

Conclusion

The results of this study lead to following conclusions:

- Although USBM and MLR-based predictor equations have given acceptable results, this study reveals the superiority of ANN-based prediction of PPV in comparison to the MLR technique and USBM predictor equation.
- It is found that the distance of the measuring station from the blasting location and SD together exert a significant impact on the prediction of PPV by MLP-based neural network approach. However, CPD exerts slightly less impact than distance and SD.
- Based on the established damage criteria of USBM, DIN 4150 and DGMS, the measured values of ground vibration (PPV) and frequency at the field were below the threshold levels, indicating them to be safe.

Conflict of interest: The authors declare no conflict of interest.

1. Uysal, O., Erarslan, K., Cebi, M. A. and Akcakoca, H., Effect of barrier holes on blast induced vibration. *Int. J. Rock Mech. Min. Sci.*, 2008, **45**(5), 712–719.
2. Ozdemir, K., Kahriman, A., Tuncer, G., Akgundogdu, A., Elver, E. and Ucan, O. N., Fragmentation assessment using a new image processing technique based on adaptive neuro fuzzy inherence systems. In Proceedings of the Annual Conference on Explosives and Blasting Technique, International Society of Explosives Engineers, 2004, vol. 2, pp. 181–188.
3. Felice, J. J., Applications of modelling to reduce vibration and airblast levels. In International Symposium on Rock Fragmentation by Blasting, Vienna, 1993, pp. 145–151.
4. Tuncer, G., Kahriman, A., Ozdemir, K., Guven, S., Ferhatoglu, A. and Gezbul, T., The damage risk evaluation of ground vibration induced by blasting in Naipli Quarry. In Third International Conference Modern Management of Mine Producing, Geology and Environmental Protection, Varna, Bulgaria, 2003, pp. 9–13.
5. Erarslan, K., Uysal, Ö., Arpaz, E. and Cebi, M. A., Barrier holes and trench application to reduce blast induced vibration in Seyitomer coal mine. *J. Environ. Geol.*, 2008, **54**(6), 1325–1331.
6. Uysal, O. and Cavus, M., Effect of a pre-split plane on the frequencies of blast induced ground vibrations. *Acta Montan. Slovaca*, 2013, **18**(2), 101–109.
7. Görgülü, K., Arpaz, E., Uysal, Ö., Durutürk, Y. S., Yüksek, A. G., Koçaslan, A. and Dilmaç, M. K., Investigation of the effects of blasting design parameters and rock properties on blast-induced ground vibrations. *Arab. J. Geosci.*, 2015, **8**(6), 4269–4278.
8. Amiri, M., Hasanipanah, M. and Amnieh, H. B., Predicting ground vibration induced by rock blasting using a novel hybrid of neural network and itemset mining. *J. Neural Comput. Appl.*, 2020, **9**, 1–9.
9. Zouari, H., Geodynamic evolution of centro meridional atlas of Tunisia. Stratigraphy, geometric analysis, cinematic and tectono-sedimentary. Ph D thesis, University of Tunis II, Tunisia, 1995.
10. Görgülü, K., Arpaz, E., Demirci, A., Koçaslan, A., Dilmaç, M. K. and Yüksek, A. G., Investigation of blast-induced ground vibrations in the Tülü boron open pit mine. *Bull. Eng. Geol. Environ.*, 2013, **72**(3–4), 555–564.
11. Ozer, U., Kahriman, A., Aksoy, M., Adiguzel, D. and Karadogan, A., The analysis of ground vibrations induced by bench blasting at Akyol quarry and practical blasting charts. *J. Environ. Geol.*, 2008, **54**(4), 737–743.
12. Azizabadi, H. R., Mansouri, H. and Fouché, O., Coupling of two methods, waveform superposition and numerical, to model blast vibration effect on slope stability in jointed rock masses. *J. Comput. Geotech.*, 2014, **61**, 42–49.
13. Saadat, M., Khandelwal, M. and Monjezi, M., An ANN-based approach to predict blast-induced ground vibration of Gol-E-Gohar iron ore mine, Iran. *J. Rock Mech. Geotech. Eng.*, 2014, **6**(1), 67–76.
14. Ambraseys, N. N. and Hendron, A. J., In *Dynamic Behaviour of Rock Masses*, John Wiley, London, 1968.
15. Langefors, U. and Kihlström, B., *The Modern Technique of Rock Blasting*, John Wiley, New York, 1978, p. 438.
16. Ghosh, A. and Daemen, J. K., A simple new blast vibration predictor of ground vibrations induced predictor. In Proceedings of the 24th US Symposium on Rock Mechanics, Texas, USA, 1983.
17. Roy, P. P., Vibration control in an opencast mine based on improved blast vibration predictors. *J. Min. Sci. Technol.*, 1991, **12**(2), 157–165.
18. Singh, V. K., Singh, D. and Singh, T. N., Prediction of strength properties of some schistose rocks from petrographic properties using artificial neural networks. *Int. J. Rock Mech. Min. Sci.*, 2001, **38**(2), 269–284.
19. Singh, T. N., Kanchan, R., Saigal, K. and Verma, A. K., Prediction of *p*-wave velocity and anisotropic property of rock using artificial neural network technique. Council of Scientific and Industrial Research, 2004.
20. Kosko, B., Neural networks and fuzzy systems: a dynamical systems approach to machine intelligence, Prentice Hall, Englewood Cliffs, NJ, 1992, p. 449.
21. Meulenkamp, F. and Grima, M. A., Application of neural networks for the prediction of the unconfined compressive strength

(UCS) from Equotip hardness. *Int. J. Rock Mech. Min. Sci*., 1999, **36**(1), 29–39.
22. Khandelwal, M. and Singh, T. N., Evaluation of blast-induced ground vibration predictors. *J. Soil Dyn. Earthq. Eng.*, 2007, **27**(2), 116–125.
23. Siskind, D. E., Structure, response and damage produced by ground vibration from surface mine blasting. US Department of the Interior, Bureau of Mines, New York, USA, 1980.
24. GSO, Vibrations in building construction. DIN 4150, German Standards Organization, Berlin, 1984.
25. Adhikari, G. R., Jain, N. K., Roy, S., Theresraj, A. I., Balachander, R., Venkatesh, H. S. and Rn, G., Control measures for ground vibration induced by blasting at coal mines and assessment of damage to surface structures. *J. Rock Mech. Tunnel. Technol*., 2006, **12**(1), 3–19.
26. Abdel-Rasoul, E. I., Measurement and analysis of the effect of ground vibrations induced by blasting at the limestone quarries of the Egyptian cement company. ICEHM 2000, Cairo University, Egypt, 2000, pp. 54–71.
27. Dowding, C. H., Suggested method for blast vibration monitoring. *Int. J. Rock Mech. Min. Geomech. Abstr.*, 1992, **29**(2), 143–156.
28. Monjezi, M., Rizi, S. H., Majd, V. J. and Khandelwal, M., Artificial neural network as a tool for backbreak prediction. *J. Geotech. Geol. Eng.*, 2014, **32**(1), 21–30.
29. Zhongya, Z. and Xiaoguang, J., Prediction of peak velocity of blasting vibration based on artificial neural network optimized by dimensionality reduction of FA-MIV. *J. Math. Prob. Eng.*, 2018, 12.
30. Lawal, A. I. and Idris, M. A., An artificial neural network-based mathematical model for the prediction of blast-induced ground vibrations. *Int. J. Environ. Stud.*, 2020, **77**(2), 318–334.
31. Leondes, C. T., Neural network systems techniques and applications. In *Advances in Theory and Applications*, Academic Press, 1998.
32. Blackwell, W. J. and Chen, F. W., *Neural Networks in Atmospheric Remote Sensing*, Artech House, 2009, pp. 78–90.
33. Nicholls, H. R., Blasting vibrations and their effects on structures. US Department of the Interior, Bureau of Mines, 1971, pp. 656–660.
34. Rorke, A. J., Blasting impact assessment for the proposed new largo colliery based on new largo mine plan 6. *J. AJR NL001 2011 Rev*., 2011.
35. Aloui, M., Bleuzen, Y., Essefi, E. and Abbes, C., Ground vibrations and air blast effects induced by blasting in open pit mines: case of Metlaoui Mining Basin, south western Tunisia. *J. Geol. Geophys.*, 2016, **5**(3), 1–8.
36. Ak, H., Iphar, M., Yavuz, M. and Konuk, A., Evaluation of ground vibration effect of blasting operations in a magnesite mine. *J. Soil Dyn. Earthq. Eng*., 2009, **29**(4), 669–676.
37. DGMS, Damage of structures due to blast induced ground vibrations in the mining area. Directorate General of Mines and Safety, Technical (S&T) Circular No. 7, 1997, pp. 9–12.

ACKNOWLEDGEMENT. We thank the staff and management of the open-cast limestone mines for their cooperation and support throughout the field work.

Received 19 January 2021; re-revised accepted 23 March 2022

doi: 10.18520/cs/v122/i11/1279-1287